

# Pyrolysis mechanism of carbon matrix precursor cyclohexane—The formation of condensed-ring aromatics and the growing process of molecules

Hui Wang<sup>a,\*</sup>, Haifeng Yang<sup>a</sup>, Wang Chuang<sup>c</sup>, Xinquan Ran<sup>a</sup>, Qizhen Shi<sup>a</sup>, Zhenyi Wen<sup>b</sup>

<sup>a</sup> Chemistry Department, Shaanxi Key Laboratory of Physico-Inorganic Chemistry, Northwest University, Xian 710069, PR China

<sup>b</sup> Institute of Modern Physics, Northwest University, Xian 710069, PR China

<sup>c</sup> School of Materials Science, Northwestern Polytechnical University, Xian 710072, PR China

Received 29 April 2006; received in revised form 26 July 2006; accepted 12 August 2006

Available online 25 September 2006

## Abstract

Based on the experiments, the UAM1 method was adopted to investigate benzene condensation of an important intermediate and the molecule growing mechanism during the cyclohexane pyrolysis process. The conclusions were drawn as follows: (1) from the viewpoint of thermodynamics, the condensation of benzene and  $C_4H_5^\bullet$  is a spontaneous reaction and the rising temperature will increase the spontaneous tendency of the reaction. (2) From the viewpoint of kinetic, the condensation of benzene and  $C_4H_5^\bullet$  is a two-step reaction. The rate-determining step is step 2 of hydrogen removal from intermediate  $C_{10}H_{10}$  (II) with the activation energy of 350.61 kJ/mol below 1473 K while the rate-determining step is step 1 that free radical  $C_4H_5^\bullet$  attacks benzene to form intermediate  $C_{10}H_{10}$  (II) with the activation energy  $\Delta E_0^{\ddagger\theta} = 31.74$  kJ/mol above 1473 K. (3) The space structure, electronic structure and thermodynamics parameters of molecular reaction of dense-ring aromatizing compounds can be used to replace the resonance energy and free valence to judge the activation of thermodynamic reaction of compounds. And (4) the analysis of the space structure, electronic structure and thermodynamic parameters show that the growing process of molecules with benzene used as initial reactants becomes more easier as the multi-ring aromatizing molecular system increases.

© 2006 Elsevier Inc. All rights reserved.

**Keywords:** Carbon/carbon composites; Cyclohexane; Pyrolysis mechanism; Condensed-ring aromatics; Aromatization; UAM1 method computation

## 1. Introduction

Among several manufacture crafts of carbon/carbon composites, the rapid liquid densification (RD) is the most economical and most efficient [1–5]. Liquid carbon matrix precursor cyclohexane is a key substance to realize the rapid densification craft. Study on the pyrolysis mechanism is beneficial for the optimization of precast parameters and the improvement of properties of the composites [6]. In the previous papers [7–11], the research group designed carefully an all-new calculation model that caters well for the study of pyrolysis mechanism of carbon matrix precursor cyclohexane through quantum chemistry calculation. With the aid of this model, the reaction mechanism of pyrolysis, condensation and aromatizing was

systematically studied theoretically, including the pyrolysis process of intermediates 1-hexene and 1,3-butadiene of cyclohexane during the primary stage, further pyrolysis of the intermediates to form C3 and C4 species, and aromatizing process to form benzene condensed from C3 and C4 species. This paper is one of the series papers concerned with the study of pyrolysis mechanism of cyclohexane. The semi-empirical quantum mechanical AM1 method was applied here to probe the growing process of molecules in the further condensation of benzene and predict the reaction tendency by thermodynamics calculation. We hope to obtain much more detail information about the pyrolysis process of cyclohexane via the systematic investigation on the pyrolysis mechanism of cyclohexane.

## 2. Design of the reaction paths

Formation of pyrocarbon is achieved by way of condensation, aromatizing, growth of rings and finally dehydrogenation

\* Corresponding author. Tel.: +86 29 88363115.

E-mail address: [huiwang@nwu.edu.cn](mailto:huiwang@nwu.edu.cn) (H. Wang).

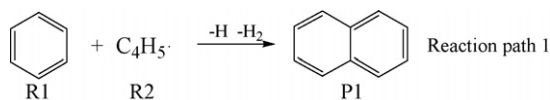


Fig. 1. The reaction path 1 of the formation of naphthalene.

of condensed-ring aromatics [12–16]. According to the present kinetic experimental research [14], benzene and free radical  $C_4H_5\bullet$  are used as initial reactants to produce naphthalene through condensation of between them. The reaction path 1 is designed as Fig. 1.

By imitating the similar mechanism as mentioned above, path 2 of the reactions of consequent ring condensation and ring growth is designed as Fig. 2. The reaction paths illustrated in this figure show the condensation reaction between the series of condensed-ring compounds numbered A–M and free radical  $C_4H_5\bullet$  or  $C_2H_3\bullet$ . In fact, the ratio of the carbon atom numbers and hydrogen atom numbers from A to M is continuously increasing, that is, hydrogen is continuously breaking away. If this process continues, dehydrogenation will proceed until forming pyrocarbon in the end.

### 3. Computation details

A semi-empirical quantum mechanical AM1 method was adopted, which is an unrestricted Hartree–Fock calculation and noted as UAM1 method in Gaussian 03 program package [17]. Geometry of reactant, intermediate, transition states and products are optimized by UAM1 method, the standard thermodynamic parameters  $\Delta E_0^\theta$ ,  $\Delta E^\theta$ ,  $\Delta H^\theta$ ,  $\Delta G^\theta$  and  $\Delta S^\theta$  for the reaction path 1 and kinetic ones  $\Delta E_0^{\neq\theta}$ ,  $\Delta E^{\neq\theta}$ ,  $\Delta H^{\neq\theta}$ ,  $\Delta G^{\neq\theta}$ ,

$\Delta S^{\neq\theta}$  and  $k$  for the transition state were derived by the following formulas [18]:

$$\Delta E_0^\theta = \Delta E_{\text{elec}}^\theta + \text{ZPE}; \quad (1)$$

$$\Delta E^\theta = \Delta E_0^\theta + \Delta E_{\text{vib}}^\theta + \Delta E_{\text{rot}}^\theta + \Delta E_{\text{trans}}^\theta \quad (2)$$

$$\Delta H^\theta = \Delta E^\theta + \Delta nRT \quad (3)$$

$$\Delta G^\theta = \Delta H^\theta - T\Delta S^\theta \quad (4)$$

where  $\Delta E^\theta$  is the energy difference between the products and the reactants under the standard condition, and ZPE is the zero-point energy correction. Similarly, we can obtain activation energies, activation enthalpy and activation free energies by subtracting the energy values of the reactants (R1 and R2) or intermediate (I1) from that of the transition states (TS1 and TS2):

$$\Delta E_0^{\neq\theta} = \Delta E_{\text{elec}}^{\neq\theta} + \text{ZPE} \quad (5)$$

$$\Delta H^{\neq\theta} = \Delta E_0^{\neq\theta} + \Delta E_{\text{vib}}^{\neq\theta} + \Delta E_{\text{rot}}^{\neq\theta} + \Delta E_{\text{trans}}^{\neq\theta} + \Delta nRT \quad (6)$$

$$\Delta G^{\neq\theta} = \Delta H^{\neq\theta} - T\Delta S^{\neq\theta} \quad (7)$$

The transition states were optimized by QST2 method and were verified by followed the frequency analyses and the IRC calculations. Here normal mode frequency analyses were performed on all stationary states and transition states. Moreover, standard thermodynamic and kinetic parameters in the range of different temperature (298, 573, 873, 1173 and 1423 K) were calculated by adding READISOTOP key word in the route section.

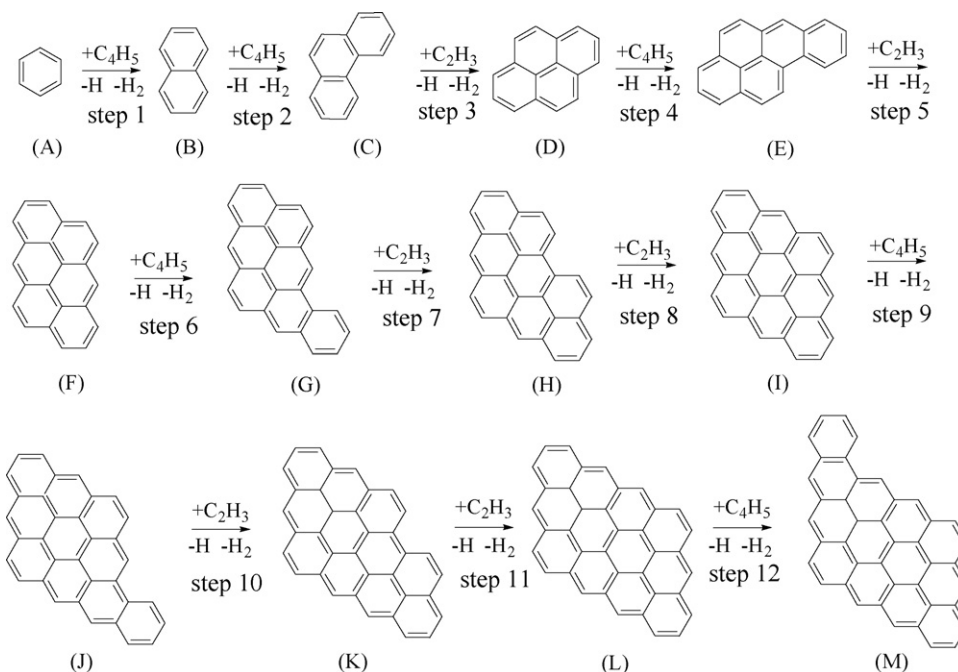


Fig. 2. The reaction path 2 of the condensed-ring aromatization process.

Based on transition state theory [19], rate constant can be calculated by the following formula:

$$k = \frac{k'T}{h} \exp\left(-\frac{\Delta G^{\ddagger\theta}}{RT}\right) = \frac{k'T}{h} \exp\left(\frac{\Delta S^{\ddagger\theta}}{R} - \frac{\Delta H^{\ddagger\theta}}{RT}\right) \quad (8)$$

where  $k'$  is the Boltzmann constant and  $h$  is the Planck constant.

All the calculations in this paper related to the application of Gaussian 03 program package are performed on Lenovo T100 Server at the Physical Chemistry Institute, Northwest University.

## 4. Results and discussion

### 4.1. Optimized geometries

The optimized bond lengths, bond angles, and dihedral angles of reactants R1 and R2 and the products (P) in the

reaction path 1 are listed in Table 1. One intermediate (I1) and two transition states TS1 and TS2 are achieved through kinetic calculation of reaction path 1 (see literature [8] for details), part of optimized parameters are also listed in Table 1. The optimized structures with marked numbers of atoms shown in Table 1 are all obtained by the UAM1 method. Data in the parentheses are the corresponding experimental ones [20], which agree well with the calculated results, proving that UAM1 method is suitable for the calculation in this paper. It can be seen from Table 1 that  $R_{(1,2)}$  bond of the product molecule P1, namely, C–C bond length approaches closely  $R_{(1,6)}$  bond length e.g. C=C length due to a large conjugated system existing in molecule P1 leading to the averaging of C–C bond length, which match well with the character of benzene. For the transition state TS1,  $R_{(5,21)}$  bond length is 0.11030 nm, a little longer than the normal C–H bond length of 0.10996 nm inside the benzene, which means

Table 1  
Part of structural parameters of reactants, products, intermediates and transition states in the naphthalene formation process (bond length, nm; bond angle/dihedral angle, degrees)

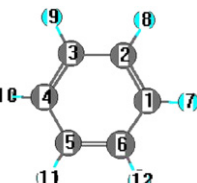
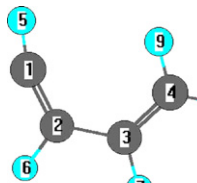

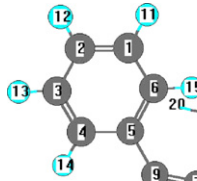
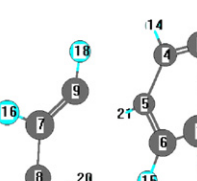
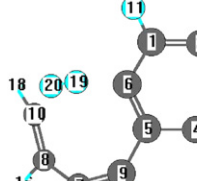
| Species  | Structural parameters   |                           |                            | Species   | Structural parameters    |                          |                           |
|--|-------------------------|---------------------------|----------------------------|---|--------------------------|--------------------------|---------------------------|
|  | Bond length             | Bond angle                | Dihedral angle             |   | Bond length              | Bond angle               | Dihedral angle            |
|   | $R_{(2,3)}$<br>0.13956  | $A_{(2,3,4)}$<br>120.00   | $D_{(6,1,2,3)}$<br>0.06    |   | $R_{(1,2)}$<br>0.13152   | $A_{(1,2,3)}$<br>126.25  | $D_{(1,2,3,4)}$<br>0.23   |
| R1   | $R_{(3,4)}$<br>0.13956  | $A_{(4,5,6)}$<br>120.00   | $D_{(6,1,2,8)}$<br>179.96  | R2  | $R_{(2,3)}$<br>0.14412   | $A_{(2,3,4)}$<br>124.72  | $D_{(1,2,3,7)}$<br>179.83 |
|  | $R_{(1,7)}$<br>0.10996  | $A_{(2,1,7)}$<br>120.00   | $D_{(2,1,6,5)}$<br>0.05    |   | $R_{(3,4)}$<br>0.13476   | $A_{(2,1,5)}$<br>179.81  | $D_{(6,2,3,4)}$<br>179.80 |
|  | $R_{(2,8)}$<br>0.10996  | $A_{(6,5,11)}$<br>120.00  | $D_{(1,2,3,9)}$<br>179.97  |   | $R_{(1,5)}$<br>0.10599   | $A_{(3,4,8)}$<br>121.85  | $D_{(2,3,4,9)}$<br>0.03   |
|  | $(R_{(3,4)} (0.1398))$  |                           |                            |   | $R_{(2,6)}$<br>0.11082   | $A_{(2,3,7)}$<br>115.20  | $D_{(7,3,4,8)}$<br>0.02   |
|  |                         |                           |                            |   |                          |                          |                           |
|  | $R_{(1,2)}$<br>0.13949  | $A_{(2,1,6)}$<br>120.52   | $D_{(6,1,2,3)}$<br>0.03    |  | $R_{(5,9)}$<br>0.14445   | $A_{(2,3,4)}$<br>120.23  | $D_{(9,7,8,10)}$<br>30.51 |
| P1   | $R_{(1,6)}$<br>0.14195  | $A_{(2,3,4)}$<br>120.35   | $D_{(2,1,6,10)}$<br>179.99 | I1  | $R_{(7,9)}$<br>0.13567   | $A_{(3,4,5)}$<br>120.56  | $D_{(2,3,4,5)}$<br>0.82   |
|  | $R_{(2,3)}$<br>0.14109  | $A_{(4,5,6)}$<br>119.13   | $D_{(3,4,5,9)}$<br>179.99  |   | $R_{(7,8)}$<br>0.14386   | $A_{(4,5,6)}$<br>118.65  | $D_{(3,4,5,9)}$<br>177.98 |
|  | $R_{(1,11)}$<br>0.10997 | $A_{(6,10,18)}$<br>118.89 | $D_{(4,5,9,7)}$<br>179.99  |   | $R_{(8,10)}$<br>0.13435  | $A_{(6,5,9)}$<br>122.44  | $D_{(6,5,9,7)}$<br>32.67  |
|  | $R_{(3,13)}$<br>0.10996 | $A_{(2,1,11)}$<br>120.59  | $D_{(5,6,10,8)}$<br>0.02   |   | $R_{(3,4)}$<br>0.13943   | $A_{(8,7,9)}$<br>129.73  | $D_{(1,2,3,4)}$<br>0.11   |
|  |                         |                           |                            |   |                          |                          |                           |
|  | $R_{(5,9)}$<br>0.21012  | $A_{(8,7,9)}$<br>129.82   | $D_{(9,7,8,10)}$<br>27.54  |  | $R_{(4,5)}$<br>0.14109   | $A_{(7,8,10)}$<br>126.12 | $D_{(6,1,2,3)}$<br>0.43   |
| TS1  | $R_{(5,21)}$<br>0.11030 | $A_{(7,8,10)}$<br>127.06  | $D_{(8,7,9,5)}$<br>3.82    | TS2   | $R_{(4,14)}$<br>0.10990  |                          |                           |
|  | $R_{(7,9)}$<br>0.13296  | $A_{(4,5,6)}$<br>118.64   | $D_{(6,5,9,7)}$<br>56.96   |   | $R_{(5,9)}$<br>0.14391   | $A_{(6,5,9)}$<br>125.49  | $D_{(9,7,8,10)}$<br>32.69 |
|  | $R_{(7,8)}$<br>0.14389  | $A_{(5,9,7)}$<br>126.03   | $D_{(4,5,9,7)}$<br>178.09  |   | $R_{(7,9)}$<br>0.1361    | $A_{(5,9,7)}$<br>130.75  | $D_{(8,7,9,5)}$<br>2.22   |
|  | $R_{(8,10)}$<br>0.13430 | $A_{(3,4,5)}$<br>120.35   | $D_{(4,5,6,1)}$<br>4.36    |   | $R_{(7,8)}$<br>0.14318   | $A_{(8,7,9)}$<br>131.20  | $D_{(4,5,9,7)}$<br>138.02 |
|  | $R_{(5,6)}$<br>0.14178  | $A_{(1,6,5)}$<br>120.35   | $D_{(3,4,5,6)}$<br>4.26    |   | $R_{(8,10)}$<br>0.13216  | $A_{(7,8,10)}$<br>128.59 | $D_{(6,5,9,7)}$<br>44.91  |
|  |                         |                           |                            |   | $R_{(19,20)}$<br>0.07477 | $A_{(4,5,6)}$<br>115.50  | $D_{(4,5,6,1)}$<br>1.33   |
|  |                         |                           |                            |   |                          |                          |                           |

Table 2

Thermodynamic parameters of the formation process of naphthalene ( $\Delta E_0^{\theta}$ ,  $\Delta E^{\theta}$ ,  $\Delta H^{\theta}$ ,  $\Delta G^{\theta}$ : kJ/mol;  $\Delta S^{\theta}$ : kJ/mol K)

| Reaction path | Parameter             | Temperature (K) |        |        |        |         |
|---------------|-----------------------|-----------------|--------|--------|--------|---------|
|               |                       | 298             | 573    | 873    | 1173   | 1473    |
| 1             | $\Delta E_0^{\theta}$ | −80.20          | −80.20 | −80.20 | −80.20 | −80.20  |
|               | $\Delta E^{\theta}$   | −78.70          | −75.42 | −72.94 | −71.69 | −71.44  |
|               | $\Delta H^{\theta}$   | −74.86          | −70.66 | −65.68 | −61.92 | −59.19  |
|               | $\Delta G^{\theta}$   | −76.59          | −81.53 | −88.39 | −96.81 | −106.08 |
|               | $\Delta S^{\theta}$   | 0.0058          | 0.0191 | 0.0260 | 0.0297 | 0.0319  |

\*  $\Delta E_0^{\theta}$  is an internal energy change of reaction path 1 in absolute zero.

that broken tendency exists attacked by free radical R2. On the other hand, as to I1,  $R_{(6,15)}$  and  $R_{(10,20)}$  are 0.11009 and 0.11089 nm, respectively, both of which are larger than C–H bond length of R1 or inside I1 ring, which implies that these two chemical bonds tend easily to break in further reactions. For transition state TS2,  $R_{(19,20)}$  reads 0.07477 nm, a little bit longer than H–H bond length, illustrating the two hydrogen atoms tend to combine.

#### 4.2. Thermodynamics analysis of the formation process of naphthalene

Thermodynamics parameters of the reaction illustrated in Fig. 1 are given in Table 2. We can conclude from the table that  $\Delta H^{\theta}$  of this path is always negative at all temperatures. In other words, it is an exothermic reaction because of the condensation

of free radicals along this path. Influenced by the entropy effect,  $\Delta G^{\theta}$  of the path reduces gradually with the temperature rising, revealing high temperature is favorable to this condensation process.

#### 4.3. Kinetic analysis of the formation process of naphthalene

The reaction mechanism in detail by kinetic calculation is shown in Fig. 3. The kinetic parameters in this process are seen in Table 3. Fig. 4 reveals the energy relationships between different standing points in the condensation process of benzene and free radical  $C_4H_5^{\bullet}$ . As shown in Fig. 3, the reaction of formation naphthalene is a two-step reaction process via an intermediate. First, free radical  $C_4H_5^{\bullet}$  attacks benzene, and then producing transition state, transferring hydrogen and forming an intermediate I1 at the same time, during which the activation energy is  $\Delta E_0^{\theta} = 31.74$  kJ/mol. Step 2 shows hydrogen removal from two carbon atoms inside I1 with activation energy  $\Delta E_0^{\theta} = 350.61$  kJ/mol, and finally forming products P1 and  $H_2$ . It is obviously from Fig. 4 that step 2 must pass over a higher energy barrier, so it is the rate-determining step during the whole process.

Strictly speaking, activation energy is the function of temperature, so it is incomplete or imperfect only to use activation energy  $\Delta E_0^{\theta}$  to explain the mechanism of Fig. 3 without consideration the influence by temperature. The reaction constant rate  $k$  is used here to discuss the reaction mechanism of the formation process of naphthalene after taking

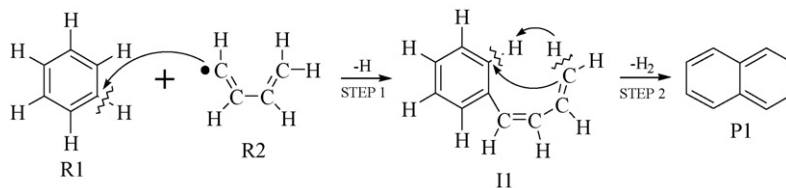


Fig. 3. Specific reaction paths of the formation process of naphthalene derived by computation (the C atom on radical site attacks the C atom of benzene indicated by the curved arrow, the C–H bond is broken by the polyline without arrow shown).

Table 3

Kinetic parameters of the formation process of naphthalene ( $\Delta E_0^{\theta}$ ,  $\Delta E^{\theta}$ ,  $\Delta H^{\theta}$ ,  $\Delta G^{\theta}$ : kJ/mol;  $\Delta S^{\theta}$ : kJ/mol K;  $k$ :  $S^{-1}$ )

| Reaction step | Parameter             | Temperature (K)        |                        |                       |                       |                    |
|---------------|-----------------------|------------------------|------------------------|-----------------------|-----------------------|--------------------|
|               |                       | 298                    | 573                    | 873                   | 1173                  | 1473               |
| 1             | $\Delta E_0^{\theta}$ | 31.74                  | 31.74                  | 31.74                 | 31.74                 | 31.74              |
|               | $\Delta E^{\theta}$   | 33.17                  | 37.17                  | 42.11                 | 47.18                 | 52.33              |
|               | $\Delta H^{\theta}$   | 30.69                  | 32.41                  | 34.84                 | 37.45                 | 40.08              |
|               | $\Delta G^{\theta}$   | 79.29                  | 123.54                 | 170.70                | 216.98                | 262.58             |
|               | $\Delta S^{\theta}$   | −0.1629                | −0.1588                | −0.1554               | −0.1529               | −0.1509            |
|               | $k$                   | $7.96 \times 10^{-2}$  | $6.57 \times 10^1$     | $1.12 \times 10^3$    | $5.33 \times 10^3$    | $1.50 \times 10^4$ |
| 2             | $\Delta E_0^{\theta}$ | 350.61                 | 350.61                 | 350.61                | 350.61                | 350.61             |
|               | $\Delta E^{\theta}$   | 353.50                 | 358.47                 | 361.55                | 362.79                | 362.88             |
|               | $\Delta H^{\theta}$   | 353.50                 | 358.47                 | 361.55                | 362.79                | 362.88             |
|               | $\Delta G^{\theta}$   | 348.45                 | 342.02                 | 332.61                | 322.43                | 312.08             |
|               | $\Delta S^{\theta}$   | 0.0169                 | 0.0287                 | 0.0331                | 0.0343                | 0.0344             |
|               | $k$                   | $5.54 \times 10^{-49}$ | $8.05 \times 10^{-19}$ | $2.30 \times 10^{-7}$ | $1.07 \times 10^{-1}$ | $2.64 \times 10^2$ |

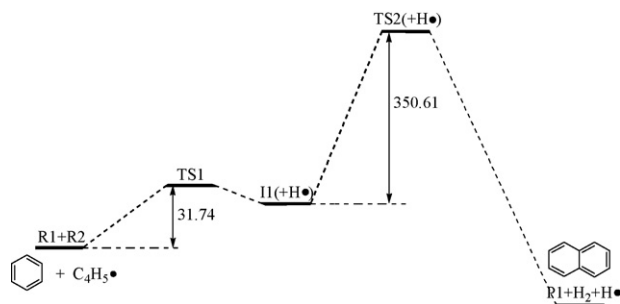


Fig. 4. Energy relationship of the standing points of the formation process of naphthalene (kJ/mol).

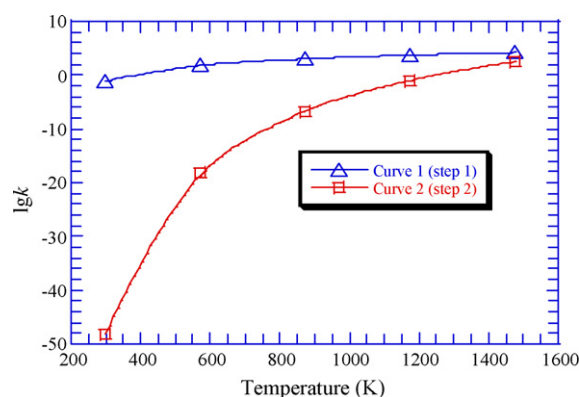


Fig. 5.  $\lg k$  variation of steps 1 and 2 vs. temperature.

into account the influence of temperature. For object seeing, we use the theory of the transition states to calculate the constant rates  $k$  of each step at different temperatures, and the variation of  $\lg k$  versus temperature is shown in Fig. 5. It can be seen from the figure that temperature exerts a little influence on step 1 such that curve 1 appears a extremely smooth tendency, namely,  $\lg k$  slightly increasing with the temperature rises. However, for step 2, curve 2 represents a greatly increasing tendency, revealing that the reaction rate of step 2 greatly improves as the temperature rises. It can be found that curve 1 is always above curve 2 at different temperature ranges below 1473 K, which means that the rate-determining step is step 2. When the temperature reaches 1473 K, the constant rate of step 2 is closely near that of step 1, which reveals that the rate-determining step may possibly become step 1 when the temperature is above 1473 K.

By analysis mentioned above, we know about the reaction mechanism in the formation process of naphthalene. What regulations would occur with the increasing carbon atom numbers if the consequent condensation reactions still follow the similar mechanism? The following research will give you an answer.

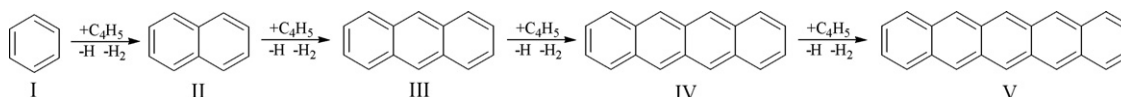


Fig. 6. One reaction path in the ring condensation process of benzene.

Table 4

DRE, Fr, average C–H bond length, average C–H bonding Mulliken population of the compounds in the ring condensation process of benzene

|                             | Compounds                     |                                |                                 |                                 |                                 |
|-----------------------------|-------------------------------|--------------------------------|---------------------------------|---------------------------------|---------------------------------|
|                             | I                             | II                             | III                             | IV                              | V                               |
| Molecular formula           | C <sub>6</sub> H <sub>6</sub> | C <sub>10</sub> H <sub>8</sub> | C <sub>14</sub> H <sub>10</sub> | C <sub>18</sub> H <sub>12</sub> | C <sub>22</sub> H <sub>14</sub> |
| DRE (eV) [23a]              | 0.869                         | 1.323                          | 1.600                           | 1.822                           | –                               |
| Fr [23b]                    | 0.399                         | 0.452                          | 0.520                           | 0.530                           | 0.540                           |
| Bonding mulliken population | 0.376874                      | 0.376761                       | 0.375773                        | 0.375583                        | 0.375360                        |
| Bond length (nm)            | 0.10996                       | 0.10996                        | 0.10996                         | 0.10996                         | 0.10997                         |

#### 4.4. Characterization parameters of thermal reaction activation in the molecular growing process

The thermal reaction activation of multi-ring aromatics compounds may be roughly concluded through Dewar resonance energy (DRE) [21] and free valence (Fr) [22].

The calculated formula for Dewar resonance energy is  $DRE = \Delta H_f^{loc} - \Delta H_f$ , where  $\Delta H_f^{loc} = 7.3435 \times C$  (the number of atoms of carbon)  $- 0.605 \times H$  (the number of atoms of hydrogen) is an energy item caused by parts of electronic delocalization in aromatics molecules,  $\Delta H_f$  is the formation enthalpy of the aromatics compound. Generally, DRE is a driving force for multi-ring aromatics molecule formed by condensed smaller aromatics molecules. The larger the DRE is, the large the value of  $\Delta H_f^{loc}$  is, which is to say the more effective the electronic delocalization inside the molecule is. This leads to the larger thermal reaction activation in aromatics molecules. Free valence (Fr) refers to the difference between the maximum bonding ( $N_{max}$ ) and the real bonding numbers ( $N_r$ ) for designated carbon atom. It shows the potential bonding capacity of carbon atoms. For a designated atom, the larger the Fr is, the larger the thermal reaction activation expected is.

In the previous research [6,7,19] we found that thermodynamics parameters of the molecular reactions, molecular space and electronic structures can be used as the basis of evaluating the thermal reaction activation of the compounds, the conclusions from which are in accordance with that judged by using DRE and free valence. Here is the proof: we calculated DRE, free valence, average C–H bonding Mulliken population, average C–H bond length of different compounds from I to V and thermodynamics parameters of various steps from steps I–II to IV–V for the condensed ring process in Fig. 6. The results are listed in Tables 4 and 5, respectively.

The some results are found regularly from the two tables. As listed in Table 4, DRE of the compound increases with the ring numbers of multi-ring aromatics compounds, and the free valence of carbon bonded with hydrogen atom increases too, showing the reaction activation increases. From the viewpoint



Table 5

Thermodynamics parameters of the steps in the ring condensation process of benzene ( $\Delta E_0^\theta$ ,  $\Delta E^\theta$ ,  $\Delta H^\theta$ ,  $\Delta G^\theta$ : kJ/mol;  $\Delta S^\theta$ : kJ/mol K)

|                     | Reaction   |              |              |            |
|---------------------|------------|--------------|--------------|------------|
|                     | Steps I–II | Steps II–III | Steps III–IV | Steps IV–V |
| $\Delta E_0^\theta$ | –80.20     | –81.86       | –83.70       | –84.18     |
| $\Delta E^\theta$   | –78.70     | –77.87       | –79.62       | –80.07     |
| $\Delta H^\theta$   | –74.86     | –75.39       | –77.15       | –77.59     |
| $\Delta G^\theta$   | –76.59     | –77.11       | –78.74       | –79.13     |
| $\Delta S^\theta$   | 0.0058     | 0.0058       | 0.0053       | 0.0051     |

of the structure parameters, the average C–H bond length increases with the ring numbers of the molecules, while the average C–H bonding Mulliken population decreases with the ring numbers of the molecules. It reveals that the C–H bond strength inside the molecule weakens with the increasing of ring numbers, as a result, the reaction activation in the pyrolysis steps of C–H bond increases. Furthermore, observing the thermodynamics parameters of the whole reaction process shown in Table 5, we found that the smaller the value of  $\Delta G^\theta$  is in each step, or better, the larger spontaneous tendency of the reaction is, the easier the condensation reaction of each step becomes than that of the previous step. Obviously, the discussion above has shown that the same conclusion can be obtained by means of utilizing different parameters shown in Tables 4 and 5, respectively. That is to say, the thermal reaction activation of a compound would increase with the ring numbers of multi-ring aromatics increasing and related hydrogen atoms in the compound also become easier to lose. Accordingly, we will make directly use of the structural parameters of multi-ring aromatics and relevant thermodynamics parameters of the reactions to discuss the reaction regulation related to the molecular growing process of ring aromatics in the following text.

#### 4.5. Reaction regulations in the molecular growing process

In the light of the reaction design of the molecular growing process shown in Fig. 2 mentioned in Section 2, the thermal reaction activation of C–H bond of each multi-ring aromatic

Table 7

Thermodynamic parameters at 298 K of each reaction step in the ring condensation process ( $\Delta E_0^\theta$ ,  $\Delta E^\theta$ ,  $\Delta H^\theta$ ,  $\Delta G^\theta$ : kJ/mol;  $\Delta S^\theta$ : kJ/mol K)

|                     | Reaction steps |        |        |        |        |        |
|---------------------|----------------|--------|--------|--------|--------|--------|
|                     | 1              | 2      | 3      | 4      | 5      | 6      |
| $\Delta E_0^\theta$ | –80.20         | –80.75 | –65.80 | –81.77 | –65.91 | –82.95 |
| $\Delta E^\theta$   | –78.70         | –80.45 | –63.36 | –77.56 | –63.39 | –78.69 |
| $\Delta H^\theta$   | –74.86         | –75.11 | –60.21 | –75.09 | –60.20 | –76.21 |
| $\Delta G^\theta$   | –76.59         | –76.72 | –64.09 | –77.20 | –64.19 | –78.28 |
| $\Delta S^\theta$   | 0.0058         | 0.0054 | 0.0130 | 0.0071 | 0.0134 | 0.0069 |

|                     | Reaction steps |        |        |        |        |        |
|---------------------|----------------|--------|--------|--------|--------|--------|
|                     | 7              | 8      | 9      | 10     | 11     | 12     |
| $\Delta E_0^\theta$ | –66.72         | –67.33 | –83.05 | –67.66 | –68.53 | –83.11 |
| $\Delta E^\theta$   | –62.78         | –62.68 | –78.73 | –62.99 | –62.85 | –78.75 |
| $\Delta H^\theta$   | –60.50         | –60.30 | –76.25 | –60.52 | –60.38 | –76.28 |
| $\Delta G^\theta$   | –64.30         | –64.25 | –78.33 | –64.38 | –64.30 | –78.38 |
| $\Delta S^\theta$   | 0.0161         | 0.0133 | 0.0069 | 0.0163 | 0.0131 | 0.0635 |

molecule was investigated from the viewpoints of the molecular and electronic structure. Listed in Table 6 are molecular formula, average C–H bond length and average C–H bonding Mulliken population for the series of condensed-ring compounds from B to M in Fig. 2. It is not difficult to find that the average bond length of each molecule increases slightly as carbon atom numbers increase while the corresponding bonding Mulliken population decreases in turn. It declares that the break of C–H bonds inside the molecule become more and more easier with the multiplying of the ring numbers of the aromatic molecular. This is because the improving of the electronic delocalization effect inside the ring resulted from the addition of the ring numbers activates the C–H bonds inside the molecule such that the thermal reaction activation of the compound strengthens. Now let us look at the thermodynamics parameters of the reaction process. Steps 1, 2, 4, 6, 9 and 12 shown in Fig. 2 are the condensation reactions of multi-ring aromatic molecules and  $C_4H_5^\bullet$ . It is apparent that  $\Delta G^\theta$  of the reaction gradually reduces with the ring numbers of aromatics increase, revealing that the capacity of the condensation of the compound and  $C_4H_5^\bullet$  becomes more and more stronger. Steps 3, 5, 7, 8, 10 and 11 shown in Fig. 2 are condensations of

Table 6

Molecular formula, average C–H bond length and average C–H bonding Mulliken population of various species

|                             | Species     |                |                |                |                |                |
|-----------------------------|-------------|----------------|----------------|----------------|----------------|----------------|
|                             | B           | C              | D              | E              | F              | G              |
| Molecular formula           | $C_{10}H_8$ | $C_{14}H_{10}$ | $C_{16}H_{10}$ | $C_{20}H_{12}$ | $C_{22}H_{12}$ | $C_{26}H_{14}$ |
| Bonding Mulliken population | 0.376761    | 0.376455       | 0.375744       | 0.375677       | 0.375667       | 0.375423       |
| Bond length (nm)            | 0.10996     | 0.10997        | 0.10998        | 0.10998        | 0.10998        | 0.10998        |

|                             | Species        |                |                |                |                |                |
|-----------------------------|----------------|----------------|----------------|----------------|----------------|----------------|
|                             | H              | I              | J              | K*             | L*             | M*             |
| Molecular formula           | $C_{28}H_{14}$ | $C_{30}H_{14}$ | $C_{34}H_{16}$ | $C_{36}H_{16}$ | $C_{38}H_{16}$ | $C_{42}H_{18}$ |
| Bonding Mulliken population | 0.375308       | 0.375237       | 0.375083       | –              | –              | –              |
| Bond length (nm)            | 0.10998        | 0.10998        | 0.10998        | 0.10999        | 0.10999        | 0.10999        |

\* Because the molecules are too large, bonding Mulliken population cannot be calculated.

multi-ring aromatics molecules and  $C_2H_3\bullet$ . Similarly,  $\Delta G^\theta$  of the reaction gradually decreases as the ring numbers of the multi-ring aromatics increase, predicting that the molecular growing process becomes much easier (Table 7).

Here must point out that the molecular growing process of ring aromatic compound is very complicated and also an important part of a whole process of cyclohexane pyrolysis until forming pyrocarbon. The present section is only the theoretical study of molecular growing process of multi-ring aromatics by using the structural parameters of multi-ring aromatics and relevant thermodynamics parameters of the reactions. Further specific research must depend on the experimental results.

## 5. Conclusion

The semi-empirical UAM1 method was applied in this paper to probe the condensation process to form naphthalene via two important intermediates aromatization between  $C_4H_5\bullet$  and benzene and to form multi-ring aromatic compound via subsequent ring condensation and growth during the cyclohexane pyrolysis process. Following conclusions were drawn:

- (1) From the viewpoint of thermodynamics, the condensation of benzene and  $C_4H_5\bullet$  is a spontaneous reaction, and the spontaneous tendency will increase as temperature rises.
- (2) From the viewpoint of kinetic, the condensation of benzene and  $C_4H_5\bullet$  is a two-step reaction. The rate-determining step is step 2 with the activation energy of 350.61 kJ/mol when the temperature is below 1473 K while the rate-determining step is step 1 with the activation energy of 31.74 kJ/mol when the temperature is over 1473 K.
- (3) The average C–H bond length and average C–H bonding Mulliken population of the multi-ring aromatic compounds as well as the thermodynamics parameters of the reaction can be used to take the place of DRE and free valence to judge the thermal reaction activation of the multi-ring aromatic compounds.
- (4) The analysis of the average C–H bond length and average C–H bonding Mulliken population of the multi-ring aromatic compounds shows that the molecular growing process to use benzene as initial reactant will proceed more easily as the molecular system of multi-ring aromatics increases.

## Acknowledgments

This work was supported by the Natural Science Foundation of Shaanxi Province. The breeding industrialized fund of the education committee of Shaanxi Province is gratefully acknowledged as well.

## References

- [1] E. Bruneton, B. Narcy, A. Oberlin, Carbon 35 (1997) 1593–1598.
- [2] M. Houdayer (Paris, FR), J. Spitz (Gieres, FR), D. Tran-Van (Brignoud, FR), United States Patent No. 4472454, 1984.
- [3] D.T. Scaringella (Littleton, MA), D.E. Connors Jr. (Nashua, NH), G.S. Thurston (Lowell, MA), United States Patent No. 5547717, 1996.
- [4] G.S. Thurston (Lowell, MA), R.J. Suplinskas (Haverhill, MA), T.J. Carroll (Salem, NH), D.F. Connors Jr. (Tewksburg, MA), D.T. Scaringella (Franklin, MA), R.C. Krutenat (Belmont, MA), United States Patent No. 5389152, 1995.
- [5] G.S. Thurston (Lowell, MA), R.J. Suplinskas (Haverhill, MA), T.J. Carroll (Salem, NH), D.F. Connors Jr. (Tewksbury, MA), D.T. Scaringella (Franklin, MA), R.C. Krutena (Belmont, MA), United States Patent No. 5733611, 1998.
- [6] Q.Z. Shi, H. Wang, Q.Z. Ran, Z.Y. Weng, Carbon/carbon composites prepared by a densification technology of rapid liquid-phase deposition and its microstructure, J. Northwest Univ. (Nat. Sci. Ed.) 32 (2002) 325–328.
- [7] H. Wang, H.F. Yang, X.Q. Ran, Q.Z. Shi, Z.Y. Weng, J. Mol. Struct. (Theochem.) 571 (2001) 115–131.
- [8] H. Wang, H.F. Yang, X.Q. Ran, Q.Z. Shi, Z.Y. Weng, J. Mol. Struct. (Theochem.) 581 (2002) 187–194.
- [9] H. Wang, H.F. Yang, X.Q. Ran, Q.Z. Shi, Z.Y. Weng, J. Mol. Struct. (Theochem.) 710 (2004) 179–191.
- [10] H.F. Yang, H. Wang, X.Q. Ran, Q.Z. Shi, Z.Y. Weng, J. Mol. Struct. (Theochem.) 618 (2002) 209–217.
- [11] H. Wang, H.F. Yang, X.Q. Ran, Q.Z. Shi, Z.Y. Weng, J. Mol. Struct. (Theochem.) 678 (2004) 39–48.
- [12] W. Benzinger, A. Becker, K.J. Huttinger, Carbon 34 (1996) 957–966.
- [13] A. Becker, K.J. Huttinger, Carbon 36 (1998) 177–199.
- [14] A. Becker, K.J. Huttinger, Carbon 36 (1998) 201–211.
- [15] A. Becker, K.J. Huttinger, Carbon 36 (1998) 213–224.
- [16] A. Becker, K.J. Huttinger, Carbon 36 (1998) 225–232.
- [17] M.J. Frisch, G.W.H. Trucks, B. Schlegel, G.E. Scuseria, M.A. Robb, J.R. Cheeseman, J.A. Montgomery Jr., T. Vreven, K.N. Kudin, J.C. Burant, J.M. Millam, S.S. Iyengar, J. Tomasi, V. Barone, B. Mennucci, M. Cossi, G. Scalmani, N. Rega, G.A. Petersson, H. Nakatsuji, M. Hada, M. Ehara, K. Toyota, R. Fukuda, J. Hasegawa, M. Ishida, T. Nakajima, Y. Honda, O. Kitao, H. Nakai, M. Klene, X. Li, J.E. Knox, H.P. Hratchian, J.B. Cross, C. Adamo, J. Jaramillo, R. Gomperts, R.E. Stratmann, O. Yazyev, A.J. Austin, R. Cammi, C. Pomelli, J.W. Ochterski, P.Y. Ayala, K. Morokuma, G.A. Voth, P. Salvador, J.J. Dannenberg, V.G. Zakrzewski, S. Dapprich, A.D. Daniels, M.C. Strain, O. Farkas, D.K. Malick, A.D. Rabuck, K. Raghavachari, J.B. Foresman, J.V. Ortiz, Q. Cui, A.G. Baboul, S. Clifford, J. Cioslowski, B.B. Stefanov, G. Liu, A. Liashenko, P. Piskorz, I. Komaromi, R.L. Martin, D.J. Fox, T. Keith, M.A. Al-Laham, C.Y. Peng, A. Nanayakkara, M. Challacombe, P.M.W. Gill, B. Johnson, W. Chen, M.W. Wong, C. Gonzalez, J.A. Pople, Gaussian 03, Revision B.01, Gaussian Inc., Pittsburgh, PA, 2003.
- [18] A. Frisch, M.J. Frisch, Gaussian98 User's Reference, second ed., 1999, p. 86.
- [19] X.C. Fu, R.H. Chen, Physical Chemistry, vol. 2, People Education Press, Beijing, 1982, pp. 235–236, 228–236 (Chinese).
- [20] R.L. David (Editor-in-Chief), CRC Handbook of Chemistry and Physics, 77rd ed., 1996–1997, pp. 5–29.
- [21] M.J.S. Dewar, H.N. Schmeising, Tetrahedron 11 (1–2) (1960) 96–120.
- [22] T. Yokono, K. Miyazawa, Y. Sanada, H. Marsh, Fuel 58 (9) (1979) 692–694.
- [23] (a) O. Sugirou, et al., Translated by LAN-ZHOU Charcoal Research Institute, Introduction to Carbonization Engineering (Chemical Industry of Carbon), Lan-Zhou: (inside exchange), 1985, pp. 85–88;  
(b) O. Sugirou, et al., Translated by LAN-ZHOU Charcoal Research Institute, Introduction to Carbonization Engineering (Chemical Industry of Carbon), Lan-Zhou: (inside exchange), 1985, p. 26.